01 Mar 1989

ANSERLIN. A Broad-Band, Low-Profile, Circularly Polarized Antenna

James L. Drewniak
Missouri University of Science and Technology, drewniak@mst.edu

P. E. Mayes

Recommended Citation

J. L. Drewniak and P. E. Mayes, "ANSERLIN. A Broad-Band, Low-Profile, Circularly Polarized Antenna," *IEEE Transactions on Antennas and Propagation*, vol. 37, no. 3, pp. 281-288, Institute of Electrical and Electronics Engineers (IEEE), Mar 1989.
The definitive version is available at https://doi.org/10.1109/8.18723

ANSERLIN: A Broad-Band, Low-Profile, Circularly Polarized Antenna

JAMES L. DREWNIAK, STUDENT MEMBER, IEEE, AND PAUL E. MAYES, FELLOW, IEEE

Abstract—**A low-profile, circularly polarized (CP) antenna can be made using an annular sector of strip conductor over a ground plane. It is simple to construct and feed. Both senses of circular polarization can be transmitted or received from the same structure. The antenna has a very wide impedance bandwidth. A figure of merit, proportional to the broadside power gain, is slowly varying over a 30 percent bandwidth. Design parameters are given for an antenna that will produce a broadside axial ratio that is less than 0.5 dB at a specified frequency.**

I. INTRODUCTION

IN RECENT YEARS the number of systems that use circularly polarized (CP) waves has been increasing. A low-profile antenna is often preferred for use on vehicles, particularly those of high speed. Several types of low-profile CP antennas are available: 1) microstrip patches [1], [2], 2) cavity-backed planar spirals [3], [4], 3) orthogonal slots [5]–[7], and curved, traveling-wave lines [8]–[10], but each has deficiencies.

A microstrip patch with a single feed point can be made to operate in a CP mode in several ways [2]; however, such antennas depend upon proper adjustment of two high-Q resonant modes and are inherently very narrow band. The bandwidth can be extended somewhat by using multiple feedpoints, or a distributed feed on a single patch [11], [12], or by using several patches in an array [13], but at the expense of a complex feeding system. Unidirectional, cavity-backed, planar spiral antennas provide much wider bandwidths; however, absorbing cavities reduce the efficiency and produce structures that are very thick in wavelengths [3], [4]. Curved, open transmission lines with traveling-wave fields have also been shown to produce CP radiation over appreciable bandwidths [8]–[10]; however, the broadside axial ratio (AR) is significantly greater than 1 dB over most of the bandwidth of these antennas.

In this paper we present a technique for improving the performance of low-profile, CP radiating-line antennas. Using this technique, the impedance bandwidth becomes so large that it no longer has any bearing on the operating bandwidth. Instead, the pattern shape and AR become the factors that limit the bandwidth. The essential elements of the technique pertain to establishing a single traveling wave on an annular sector of conducting strip that is positioned parallel and close to a large conducting surface. The antenna is named the annular sector, radiating-line (ANSERLIN) antenna.

Planar and conical log-spiral antennas in free space are known to produce CP radiation with a small AR over most of the main beam [3], [14]. The on-axis CP radiation from these antennas is attributed to a near field with an azimuthally traveling wave with a phase shift of one degree per degree of transversal in azimuth [15]. The angular dependence of Maxwellian fields in systems with no boundaries on the azimuthal angle ϕ can be expressed as $e^{\pm jm\phi}$ where m must be an integer. The on-axis far-zone fields are nonzero only when $m = 1$. Results from [16] show that a traveling-wave electric current loop with one degree of phase shift per degree angle of traversal along the loop produces a radiation pattern in which the $m = 1$ mode is the dominant contributor to the far field. This paper describes how an annular sector of strip conductor over ground can form a transmission-line antenna with a traveling-wave phase shift of one degree per degree of traversal on the annular sector. Henceforth, the ratio of the near-field phase shift to the corresponding increment in the azimuthal angle will be designated by m'. The ANSERLIN antenna then operates over a band of frequencies in which $m' \cong 1$.

Experimental results for two-port ANSERLIN antennas are presented. The method of exciting a traveling wave on the annular sector is discussed. The ANSERLIN antenna is shown to have a very wide impedance bandwidth. This is a consequence of the method used to maintain a constant impedance along the structure from the input port to the output port. The frequency at which a phase shift of $m' = 1$ is achieved will be given. For a phase shift of $m' = 1$, the ANSERLIN antenna produces a predominantly $m = 1$ mode radiation pattern. By varying the phase shift about $m' = 1$, the antenna is shown to have a wide radiation pattern bandwidth over which a low value of AR is achieved over most of the beam. A figure of merit that is proportional to the power gain at broadside is shown to be slowly varying over a 30 percent bandwidth. For one set of geometric parameters 60 percent of the input power can be radiated when $m' = 1$. The percentage of input power that is radiated increases with frequency.

Either sense of CP can be transmitted or received by the two-port ANSERLIN antenna simply by feeding one port or the other and terminating the opposite port in a nonreflecting load. By adjusting the amplitude and phase of two simultaneously applied inputs, one to each port, any polarization can be achieved. A measurement of amplitudes and phases of the outputs at matched ports in a receiving situation provides a means for determining the polarization of the incident wave.

Manuscript received February 23, 1988. This work was supported by TRW.

The authors are with the Electromagnetics Laboratory, Department of Electrical and Computer Engineering, University of Illinois, Urbana-Champaign, IL 61801.

IEEE Log Number 8825063.

0018-926X/89/0300-0281$01.00

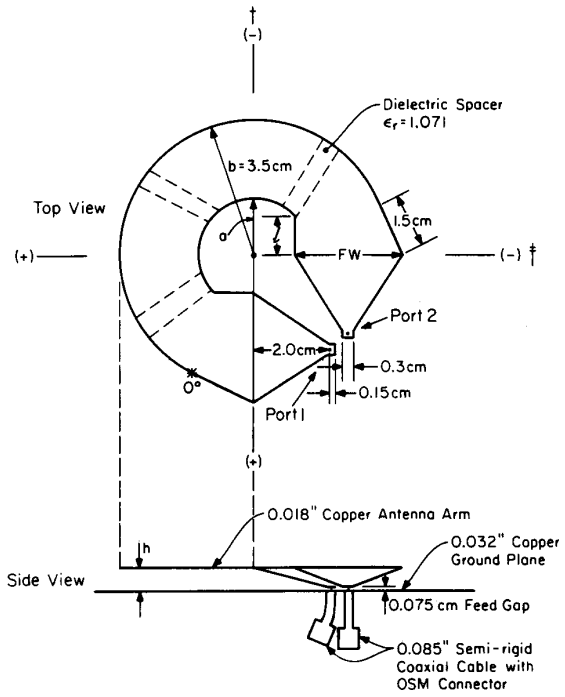

Fig. 1. Annular sector, radiating-line antenna geometry. †: Elevation plane for the radiation pattern of Fig. 5. ‡: Elevation plane for the radiation patterns of Fig. 6.

II. Annular-Sector, Radiating-Line Geometry

The method of feed is as important as the structure geometry in achieving good results. For minimum variation in impedance it is necessary to produce a pure traveling wave on the annular sector transmission line. The annular sector must be fed near one end and terminated on the other so that no reflected wave is produced. A reflected wave radiates the opposite sense of circular polarization, thereby degrading the radiation pattern performance. A method for feeding and terminating the annular sector which results in small or no end reflections is shown in Fig. 1. A fin transmission line is excited across a small feed gap by a 50 Ω, 0.085-in coaxial cable probe. The small tab on the fin at the feed point provides susceptance to tune the reactance of the feed probe. The ratio of the width w of the fin to the height h above the ground plane at any point along the length is constant. As a result, formulas for the characteristic impedance of a microstripline as a function of w/h have been found to be accurate for designing the fin. Time-domain reflectometry measurements have shown the characteristic impedance of the annular sector transmission line to be nearly constant along the length of the line; however, the w/h ratio for a 50 Ω annular sector is less than the w/h ratio for a straight, 50 Ω microstrip line. A width transition is then necessary between the end of the fin and beginning of the annular sector, as shown in Fig. 1. The output of the annular sector is identical to the input, and the output port is terminated in 50 Ω. It is not essential that the impedance of the annular sector be equal to 50 Ω, but this value was chosen in the work reported here for convenience in testing. The geometric parameters of the six antennas studied to date are given in Table I. The listed parameters are defined in Fig. 1. The antennas differ in the ratio of the outer to the inner diameter, $b/a = \Lambda$, but they were all constructed to produce an $m' = 1$ phase shift at approximately 2.0 GHz. In all cases except antenna #6, the fin was centered on the annular sector. The height above the ground plane of antenna #6 required an excessively large angle to achieve as close to 50 Ω as possible for the fin. It was therefore necessary to offset the fin 2.0 mm toward the outside edge of the annular sector.

TABLE I
ANNULAR-SECTOR, RADIATING-LINE GEOMETRY PARAMETERS

Antenna	$w = b-a$ (cm)	h (cm)	FW (cm)	ℓ (cm)	$\Lambda = \frac{b}{a}$	$\frac{w}{h}$	$\frac{FW}{h}$
1	1.5	0.35	1.7	1.0	1.75	4.3	4.8
2	2.1	0.55	2.6	1.0	2.5	3.8	4.7
3	2.3	0.65	3.0	0.8	2.92	3.5	4.6
4	2.55	0.70	3.3	0.8	3.68	3.6	4.7
5	2.7	0.8	3.8	0.8	4.38	3.4	4.7
6	3.0	1.05	4.0	0.5	7.0	2.9	3.8

The ANSERLIN antenna can be mounted flush with a larger ground surface with a cylindrical cavity surrounding the antenna, or the ground surface for the ANSERLIN antenna can be mounted on the same level with a larger ground surface. The performance of the antenna is the same in both cases. The results presented in this paper are for the annular sector mounted flush with a large ground plane. The surrounding cylindrical cavity walls are 2.0 cm from the outer edge of the annular sector.

III. Input Impedance

Time-domain reflectometry measurements have been used to ensure that the characteristic impedance of the annular sector transmission line for narrow arms ($\Lambda < 3.0$) remains constant along the length of the arm. For $\Lambda < 3.0$, the w/h ratio for a 50 Ω annular sector line varies almost linearly with Λ, as shown in Fig. 2. For $\Lambda > 3.0$, $w/h = 3.5$ provides the closest match to 50 Ω. By designing the annular sector transmission line to be 50 Ω or nearly 50 Ω, and feeding it with a 50 Ω fin, the entire transmission line from input to output is approximately 50 Ω. When Port 2 is terminated in 50 Ω, the input impedance seen at Port 1 should then be 50 Ω over a very wide bandwidth. The input impedance of antenna #4, which is typical of ANSERLIN antennas for $\Lambda < 4.0$, is shown in Fig. 3(a) over an 8:1 frequency span. The locus is compact and centered on 50 Ω. The input impedance of antenna #5 for 1.9–3.0 GHz (which encompasses the radiation pattern bandwidth) is shown in Fig. 3(b). In both cases it is clear that the return loss of the antenna can be made quite large over the radiation pattern bandwidth. For the an-

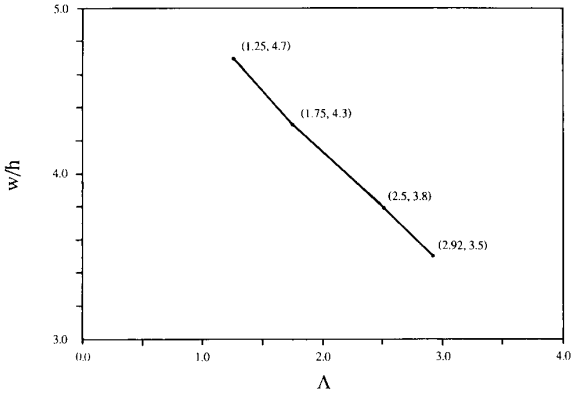

Fig. 2. w/h versus Λ for 50 Ω annular sectors.

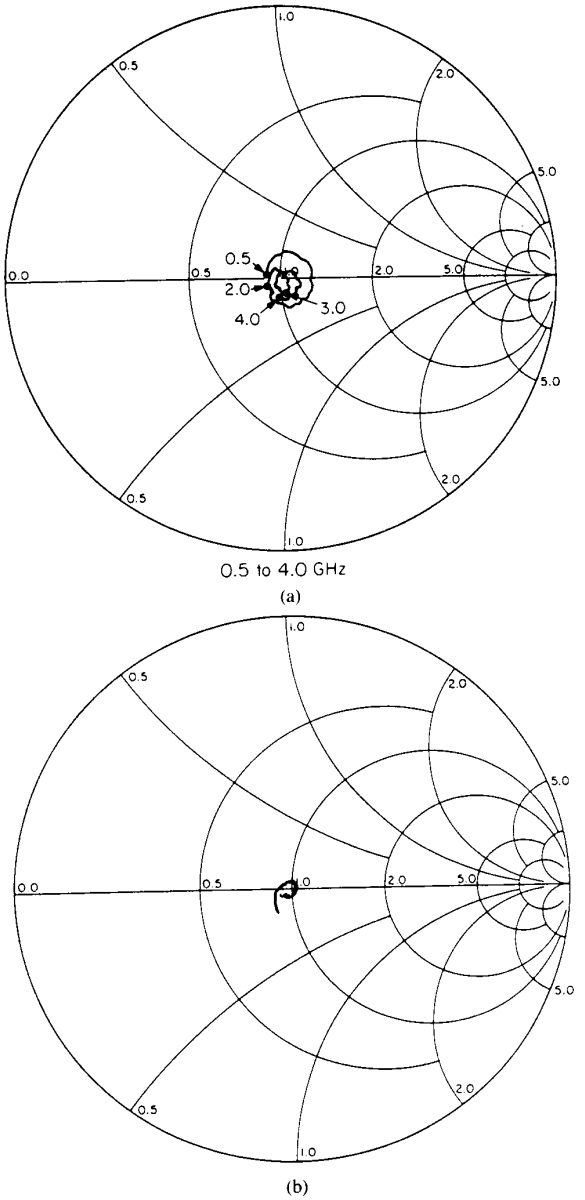

Fig. 3. Annular sector, radiating-line antenna input impedance. (a) Antenna #4, 0.5-4.0 GHz. (b) antenna #5, 1.9-3.0 GHz.

tennas of Table I, with the exception of antennas #5 and #6, greater than 25 dB return loss was measured over the radiation pattern bandwidth. Greater than 20 dB return loss over the radiation pattern bandwidth was measured for antenna #5, and greater than 18 dB return loss was measured for antenna #6. The return loss measured for antennas #5 ($\Lambda = 4.38$) and #6 ($\Lambda = 7.0$) has been observed to be less sensitive to w/h of the annular sector (for sufficiently matched fins) than for a narrow width of the annular sector. For $\Lambda = 7.0$, the return loss from 1.9–2.4 GHz changes from greater than 25 dB for $w/h = 3.33$ to greater than 20 dB for $w/h = 2.86$. The increase in volume for the increase in h; however, results in a 6 percent increase in the percentage of the input power that is radiated for $w/h = 2.86$ as compared with $w/h = 3.33$.

IV. Characteristics of the Annular Sector, Radiating Line

A quasi-transverse electromagnetic (TEM), traveling wave has been assumed for the fields beneath the annular sector. The phase variation of the electric field was measured to test the validity of this assumption. The antenna was fed at Port 1 (Fig. 1) and terminated in a 50 Ω load at Port 2. The phase of the electric field was then sampled with a short monopole probe by performing S_{21} measurements between Port 1 and the probe using the HP8510 network analyzer. The results of the relative phase measurements at 2.1 GHz are plotted in Fig. 4 for the phase along the outside edge of the annular sector. The 0° point on the annular sector is denoted by an asterisk in Fig. 1. The reference plane for $\angle S_{21}$ is the input terminal of the fin transmission line.

From Fig. 4 it is clear that the phase progression along the annular sector is that of a traveling wave, $e^{-j\beta s}$, where s is the arc length and β is the phase constant. Substituting for the arc length, $s = r\phi$,

$$e^{-j\beta s} = e^{-j\beta r\phi} = e^{-jm'\phi} \tag{1}$$

where m' is defined as

$$m' = \beta r. \tag{2}$$

The phase variation of the mth circularly polarized mode in free space is $e^{-jm\phi}$. Thus the ANSERLIN antenna should have a predominantly $m = 1$ circularly polarized mode radiation pattern at the frequency for which $m' = 1$. Furthermore, the radiation pattern should be dominated by the $m = 1$ mode for variations in m' about unity. It is the allowable variation of m' about unity that produces that much wider CP bandwidth of the ANSERLIN antenna as compared with the CP resonant microstrip patch antenna.

The phase was also measured across width of the annular sector, and the equiphase contours were observed to be nearly radial lines. The radial equiphase contours together with (2) suggests a manner in which the $m' = 1$ frequency can be approximated. By taking β as the free-space phase constant and $\langle r \rangle = (a + b)/2$, an expression for the $m' = 1$ frequency can be obtained from (2)

$$f = \frac{c}{2\pi\langle r \rangle} m' \tag{3}$$

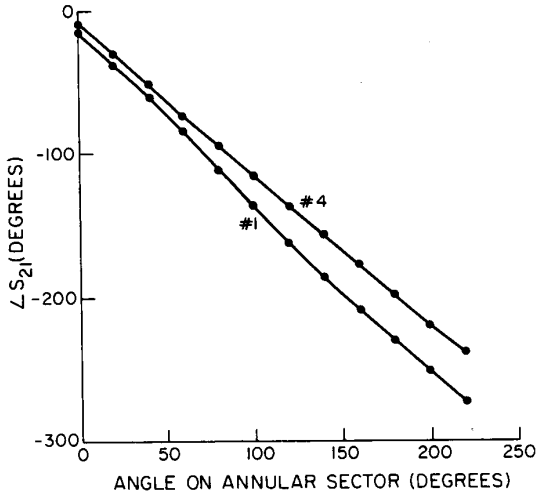

Fig. 4. Relative phase measurements at 2.1 GHz on the outside edge of the annular sector for antennas #1 and #4.

TABLE II
COMPARISON OF THE $m' \approx 1$ FREQUENCIES DETERMINED FROM RADIATION PATTERN MEASUREMENTS, $f_{(\text{patterns})}$, WITH THAT OF (3), $f_{(3)}$, AND THE PERCENTAGE OF THE INPUT POWER RADIATED AT THE $m' \approx 1$ FREQUENCY, AND AT 2.4 GHz

antenna	Λ	$f_{(\text{patterns})}$ (GHz ± 0.05 GHz)	$f_{(3)}$ (GHz)	% input power radiated	
				m' ≈ 1 frequency	2.4 GHz
1	1.75	1.75	1.74	11	20
2	2.5	2.05	1.95	30	45
3	2.92	2.10	2.03	37	52
4	3.68	2.10	2.16	43	62
5	4.38	2.10	2.22	50	71
6	7.0	2.05	2.39	60	85

where c is the free space phase velocity. The ANSERLIN antenna was observed from two-port measurements to be dispersive, as a result (3) is only approximate. The approximation can be checked from the results of Fig. 4. The magnitude of the slope of the lines in Fig. 4 is m'. The difference between m' measured at 2.1 GHz and that predicted by (3) for antenna #1 is 1 percent. For antenna #4 the difference between the measured and calculated values of m' is 5.8 percent. The approximation in the $m' = 1$ frequency given by (3) becomes worse as Λ increases because of the increasing dispersion for the thicker antennas. However, because of the large bandwidth of the antenna, (3) remains a good approximation even for antenna #5, as observed from radiation pattern measurements. The frequencies, $f_{(\text{patterns})}$, at which the radiation pattern of each of the six antennas of Table I displayed predominantly $m = 1$ mode characteristics, were determined. Table II compares $f_{(\text{patterns})}$ with the $m' = 1$ frequency approximated by (3), $f_{(3)}$. The change in the radiation pattern between the frequencies $f_{(\text{patterns})}$ and $f_{(3)}$ is small. Only for antenna #6, is the agreement poor. The thickness of antenna #6 causes it to be significantly more dispersive than the other five antennas. The approximation in (3) for antenna #6 is therefore somewhat rough, and noticeable changes occur in the radiation pattern between $f_{(\text{patterns})}$ and $f_{(3)}$.

Another characteristic of the ANSERLIN antenna is the increase in radiation loss for increasing Λ (and hence height above the ground plane for a 50 Ω input impedance). The percentage of the input power that is radiated at the $m' = 1$ frequency and at 2.4 GHz for each of the six antennas studied is listed in Table II. The $|S_{21}|$ in decibels (measured between Ports 1 and 2 of the antenna) has been measured to be nearly linear with Λ [17]. The variation of the radiation loss with

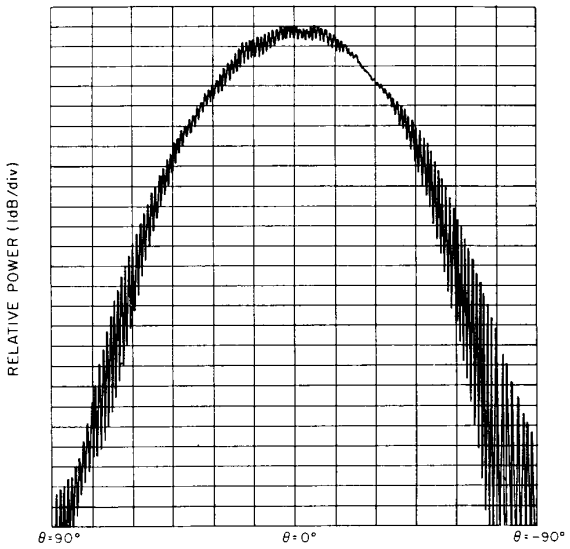

Fig. 5. Elevation plane radiation pattern of antenna #5 measured with a spinning dipole at 2.10 GHz ($m' = 1$ frequency).

element geometry, and in particular the approximate linearity of $|S_{21}|$ versus Λ indicates that the ANSERLIN element can be used to achieve a specific taper of the amplitude distribution in a series-fed array. This has been done and is presented in [17]. From Table II it is seen that the maximum percentage of the input power that is radiated by an ANSERLIN antenna so far achieved for $m' = 1$ is 60 percent.

V. Radiation Patterns

Extensive radiation patterns have been measured for each of the antennas of Table I to determine the frequency at which the radiation patterns display predominantly $m = 1$ mode characteristics, and to characterize the radiation pattern performance with varying frequency. Shown in Fig. 5 is an elevation plane pattern at 2.10 GHz for antenna #5 measured with a spinning dipole and recorded on a rectangular chart recorder. The pattern is measured in the elevation plane making a 45° angle (clockwise) with the plane of symmetry of the antenna. Because the radiation patterns are not perfectly symmetric about $\theta = 0°$ (broadside), the orientation of the radiation patterns with respect to the antenna is denoted by $\theta = \pm 90°$ for the ($\pm$) side of the antenna (Fig. 1). Fig. 5 is a typical example of the radiation patterns of ANSERLIN antennas for a phase shift of $m' = 1$. The beam is a hemispherical lobe with an average half-power beamwidth of 65°. At the frequency for which $m' = 1$, the beam is fairly symmetric about $\theta = 0°$. The axial ratio (AR) at $\theta = 0°$ is 0.5 dB. An AR of 0 dB at $\theta = 0°$ has been measured for some antennas. The AR at the half-power points is less than 2.5 dB for all antennas, and remains less than 2.5 dB for angles smaller than the half-power angles. Somewhat degraded performance was observed for antenna #1. In this case the AR is 2 dB at $\theta = 0°$, and averages 3.5 dB at the half-power points. The frequencies at which the antennas of Table I displayed predominantly $m = 1$ mode characteristics are listed in Table II.

Figs. 6(a)–6(e) show the variation of the radiation pattern of antenna #5 from 1.9–2.6 GHz. The elevation plane radiation patterns were measured with a spinning dipole in the plane making a 45° angle (counterclockwise) with the plane of symmetry of the antenna. The radiation patterns in Figs. 6(b)–6(e) were measured with the annular-sector arm mounted flush with a 36-in circular aluminum ground plane. Diffraction ripple precluded obtaining quantitative AR information at 1.9 GHz using a 36-in ground plane. The radiation pattern in Fig. 6(a) was therefore measured with the annular sector mounted over a 6-in square ground plane. The AR at $\theta = 0°$ over 2.0–2.4 GHz averages 0.5 dB for all antennas of Table I (except #1). The AR is somewhat greater at 1.9 GHz as shown in Fig. 6(a). For 2.0–2.6 GHz the AR is less than 2.5 dB at the half-power points, and remains less than 2.5 dB for angles less than the half-power angles. The half-power beamwidth narrows as the frequency is increased, decreasing from an average of 65° at 2.0 GHz, to less than 60° at 2.6 GHz.

A figure of merit that is an indication of the power gain at broadside can be determined over the 1.9–2.6 GHz frequency band measured from parameters of the radiation pattern of antenna #5 given in Table III. The figure of merit is defined by

$$P_{FM} = \left(\frac{P_{rad}}{P_{in}}\right)\left[\frac{1}{1+\left(\frac{1-AR}{1+AR}\right)^2}\right]\left(\frac{P_{OA}}{P_{MB}}\right) \quad (4)$$

where $(P_{rad}/P_{in}) \cong 1 - |S_{21}|^2$ is the total radiated power (since $|S_{11}| \cong 0$), the second factor is the fraction of power that is radiated with the desired sense of CP [18], and the third factor, P_{OA}/P_{MB}, is the ratio of power at broadside to the power at the beam maximum (to account for the squinting of the beam off broadside for $m' \neq 1$). This figure of merit does not account for the narrowing of the main beam, and growth of the sidelobe with increasing frequency; however, these two factors roughly offset one another for the frequency span measured. An artifact of the radiation pattern measurement system used in this study is the variation in the AR at $\theta = 0°$ by as much as 0.5 dB for different elevation planes, as well as an uncertainty of 0.25 dB in the power at $\theta = 0°$ relative to the beam maximum. As a result, the entries in Table III for the AR are an average of the AR for the four elevation planes measured. The entries for power relative to the beam maximum are the maximum for an uncertainty of 0.25 dB in the measurement. The figure of merit given by (4) is plotted versus frequency over a 30 percent bandwidth for antenna #5 in Fig. 7. The variation of the figure of merit versus frequency for antenna #5 is typical of all annular-sector, radiating-line antennas; however, the percentage of the input power that is radiated at a given frequency increases as the width of the annular sector is increased.

A limiting factor in the radiation pattern bandwidth of the antenna may be the squinting of the main beam from $\theta = 0°$ for frequencies at which $m' \neq 1$. The beam squint is always greatest in the plane perpendicular to the symmetry plane of the antenna. The beam squint is taken as the average of the $\pm\theta$ angles at the half-power points of the radiation pattern.

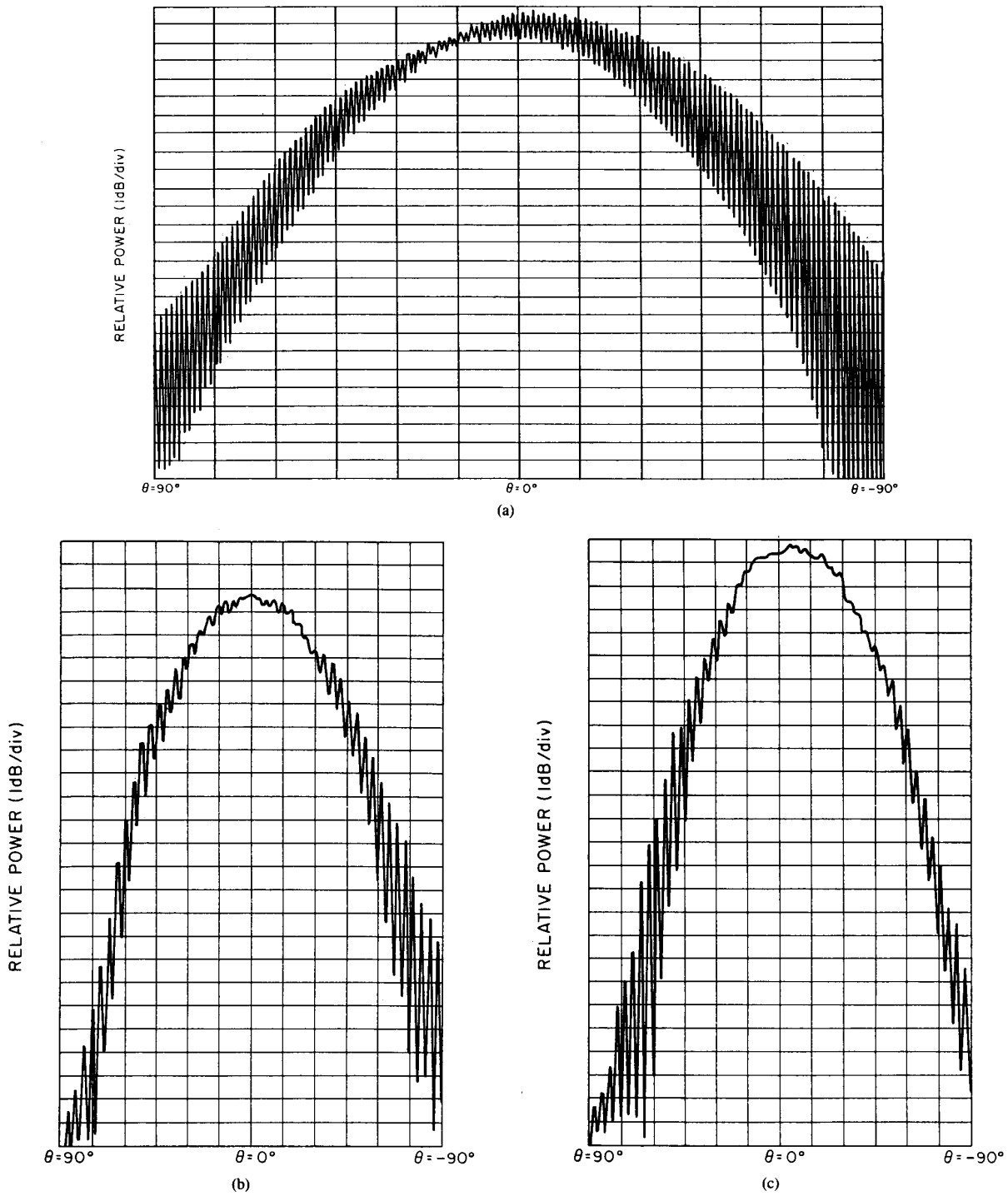

Fig. 6. Elevation plane radiation patterns of antenna #5 measured with a spinning dipole. (a) 1.9 GHz. (b) 2.0 GHz. (c) 2.2 GHz. (d) 2.4 GHz. (e) 2.6 GHz.

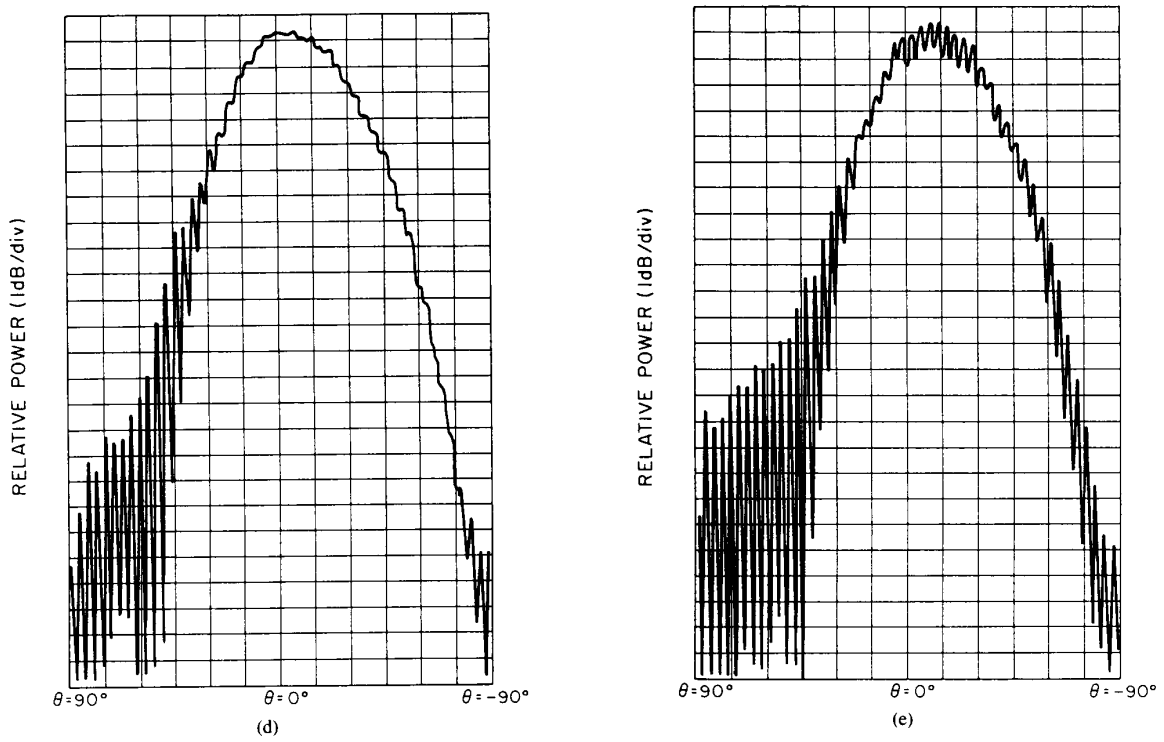

Fig. 6. (*Continued*)

TABLE III
PERCENTAGE OF THE INPUT POWER THAT IS RADIATED, AR AT $\theta = 0°$, AND POWER AT $\theta = 0°$ RELATIVE TO THE BEAM MAXIMUM FOR ANTENNA #5

frequency (GHz)	% of input power radiated $(1-\|S_{21}\|^2)$	average AR at $\theta = 0°$ (dB)	power at $\theta = 0°$ relative to the beam maximum (dB)	figure of merit (in percent)
1.9	38	1.0	-0.25	35
2.05	45	0.5	-0.25	42
2.1	50	0.5	-0.25	47
2.2	64	0.25	-0.25	60
2.4	71	0.25	-0.25	67
2.6	77	1.0	-1.0	60

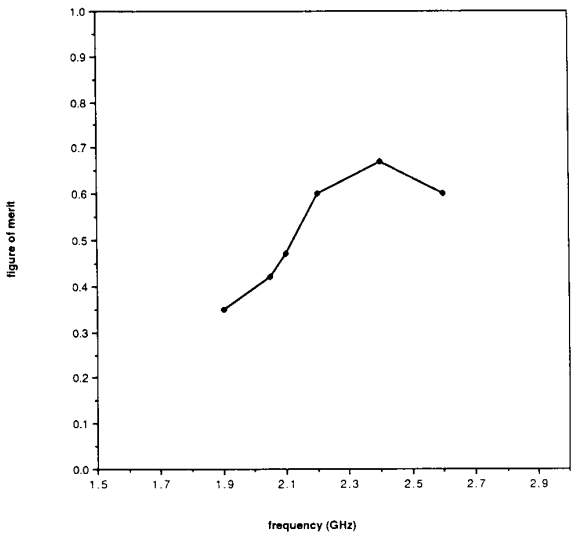

Fig. 7. A figure of merit that is indicative of the power gain at broadside as a function of frequency.

For $m' < 1$, the beam squint is toward $\theta = +90°$. For antenna #5, the beam squint is 6° at 1.9 GHz. For $m' > 1$, the beam squint is toward $\theta = -90°$, and is slightly less than 15° at 2.6 GHz for antenna #5.

V. Conclusion

A simple, low profile, traveling-wave antenna with a broadband, circularly polarized radiation pattern has been presented. The traveling-wave phase progression at the $m' \cong 1$ frequencies results in a source distribution that is known to produce a single-lobe, circularly polarized radiation pattern. A wideband 50 Ω input impedance has been shown. The traveling-wave phase shift has been verified through near-field probing measurements. An approximate formula for the $m' = 1$ frequency has also resulted from the near-field probing measurements. A wide radiation pattern bandwidth based

on a defined figure of merit has been achieved. Although an air dielectric was used for the annular sector, radiating-line antenna in this study, it should not be considered essential. However, constructing the antenna on a substrate with $\epsilon_r \neq 1$ will affect the radiation pattern performance. It is expected that the $m' = 1$ frequency will be lowered and the percentage of the input power that is radiated at a given frequency will be decreased. However, the beam broadening resulting from the lower $m' = 1$ frequency should reduce some of the effect of the beam squint. A 270° annular sector was used in this study to allow space for the input and output fin transmission lines. Feeding the annular sector in another manner that allows for an angle of larger than 270°; however, will increase the percentage of input power that is radiated by an annular sector, radiating-line antenna.

Acknowledgment

The authors gratefully acknowledge the ideas and suggestions of David Tanner in the development of this antenna. They thank James Woodruff, Robert Madland, and James Gentle for assistance in the construction of the antennas and measuring radiation patterns.

References

[1] J. K. Kerr, "Microstrip polarization techniques," in *Proc. 1978 Antenna Appl. Symp.*, Univ. Illinois, Urbana.

[2] Y. T. Lo and B. Engst, "Circularly polarized microstrip antennas," in *Proc. 1984 Antenna Appl. Symp.*, Univ. Illinois, Urbana.

[3] J. D. Dyson, "The equiangular spiral antenna," Univ. Illinois Antenna Lab., Urbana, Tech. Rep. 21, Sept. 1957.

[4] G. Grekou and G. Dubost, "Antanne spirales equiangulares planes a quatre brin a reflecteur conique et a cavete enostree dans une structure," *Electron. Lett.*, vol. 11, pp. 169–170, Apr. 1975.

[5] H. E. King and J. L. Wong, "A shallow ridged-cavity crossed-slot antenna for the 240- to 400-MHZ frequency range," *IEEE Trans. Antennas Propagat.*, vol. AP-23, pp. 687–689, Sept. 1975.

[6] A. J. Simmons, "Circularly polarized slot radiators," *IEEE Trans. Antennas Propagat.*, vol. AP-5, pp. 31–36, Jan. 1957.

[7] C. A. Lindberg, "A shallow-cavity UHF crossed-slot antenna," *IEEE Trans. Antennas Propagat.*, vol. AP-17, pp. 558–563, Sept. 1969.

[8] J. Drewniak, P. Mayes, D. Tanner, and R. Waller, "A log-spiral, radiating-line, antenna," in *IEEE Antennas Propagat. Soc. Int. Symp. Dig.*, June 1986, pp. 773–776.

[9] H. Nakano, K. Nogami, S. Arai, H. Mimaki, and J. Yamachi, "A spiral antenna backed by a conducting plane reflector," *IEEE Trans. Antennas Propagat.*, vol. AP-34, pp. 791–796, June 1986.

[10] C. Wood, "Curved microstrip lines as compact wideband circularly polarized antennas," *Inst. Elec. Eng. Microwaves, Opt. Acoust.*, vol. 3, pp. 7–13, Jan. 1979.

[11] T. Chiba, Y. Suzuki, and N. Miyano, "Suppression of higher modes and cross polarized component for microstrip antennas," *IEEE Antennas Propagat. Soc. Int. Symp. Dig.*, May 1982, pp. 285–288.

[12] B. Schnizer, W. Paschen, and R. Wohlleben, "Theoretical and experimental investigation of a torus as a primary feed in reflector antennas," presented at URSI Int. Symp. Electromagn. Theory, Budapest, Hungary, Aug. 1986.

[13] J. Huang, "A technique for an array to generate circular polarization with linearly polarized elements," *IEEE Trans. Antennas Propagat.*, vol. AP-34, pp. 1113–1124, Sept. 1986.

[14] J. D. Dyson, "The characteristics and design of the conical log-spiral antenna," Univ. Illinois Antenna Lab., Urbana, Tech. Rep. AFAL-TR-65-124, May 1965.

[15] C. S. Liang and Y. T. Lo, "A multipole-field study for the multiarm log-spiral antennas," *IEEE Trans. Antennas Propagat.*, vol. AP-16, pp. 656–664, Nov. 1968.

[16] H. L. Knudsen, "The field radiated by a ring quasi-array of an infinite number of tangential or radial dipoles," *Proc. IRE*, vol. 41, pp. 781–789, June 1953.

[17] J. Drewniak and P. E. Mayes, "Broadband, circularly polarized, radiating-line antennas with an application to a series-fed array," Univ. Illinois Electromagn. Lab., Urbana, Rep. 87-4, July 1987.

[18] V. H. Rumsey, G. A. Deschamps, M. L. Kales, and J. I. Bohnert, "Techniques for handling elliptically polarized waves with special reference to antennas," *Proc. IRE*, vol. 51, pp. 533–552, May, 1951.

James L. Drewniak (S'85) was born in Beach, ND, on July 13, 1962. He attended the University of North Dakota and received the B.S. (highest honors) and M.S. degrees in electrical engineering from the University of Illinois, Urbana-Champaign, in 1985 and 1987 respectively. He is currently pursuing a Ph.D. degree in electrical engineering.

From 1985 to 1987 he was a Graduate Research Assistant in the Electromagnetics Laboratory at the University of Illinois investigating broad-band, circularly polarized, radiating-line antennas. Currently he is a Graduate Research Assistant in the Bioacoustics Laboratory at the University of Illinois. His research is in the area of ultrasonic tissue characterization, and ultrasonic biological effects.

Mr. Drewniak is a member of Eta Kappa Nu and Tau Beta Pi.

Paul E. Mayes (S'50–M'51–SM'71–F'75) was born in Frederick, OK, on December 21, 1928. He received the B.S.E.E. degree from the University of Oklahoma, Norman, in 1950 and the M.S.E.E. and Ph.D. degrees from Northwestern University, Evanston, IL, in 1952 and 1955, respectively.

From 1950 to 1954 he was employed as a Graduate Assistant and Research Associate in the Microwave Laboratory at Northwestern where his research was on electromagnetic wave propagation along dielectric rod waveguides and reflection of electromagnetic waves from curved conducting surfaces. Since 1954 he has been on the faculty of the Department of Electrical Engineering, University of Illinois, Urbana-Champaign, where he is now a Professor teaching courses in electromagnetic theory and antennas and supervising research in the Electromagnetics Laboratory. His research at Illinois has been concerned with low-profile antennas, numerical electromagnetic analysis, microwave transmission lines, and frequency-independent antennas.

Dr. Mayes was an elected IEEE Fellow in 1975 for "contributions to the theory and development of the log-periodic antennas." He has served as technical consultant to industry and has 11 patents on antenna inventions. He is a member of Sigma Xi, Tau Beta Pi, and Eta Kappa Nu.